THE ASTROPHYSICAL JOURNAL, 529:L103–L106, 2000 February 1
© 2000. The American Astronomical Society. All rights reserved. Printed in U.S.A.

POPULATION OF THE SCATTERED KUIPER BELT[1]

CHADWICK A. TRUJILLO AND DAVID C. JEWITT
Institute for Astronomy, 2680 Woodlawn Drive, Honolulu, HI 96822; chad@ifa.hawaii.edu, jewitt@ifa.hawaii.edu
AND
JANE X. LUU
Leiden Observatory, P.O. Box 9513, 2300 RA Leiden, The Netherlands; luu@strw.leidenuniv.nl
Received 1999 October 27; accepted 1999 December 6; published 1999 December 30

ABSTRACT

We present the discovery of three new scattered Kuiper Belt objects (SKBOs) from a wide-field survey of the ecliptic. This continuing survey has to date covered 20.2 deg^2 to a limiting red magnitude of 23.6. We combine the data from this new survey with an existing survey conducted at the University of Hawaii 2.2 m telescope to constrain the number and mass of the SKBOs. The SKBOs are characterized by large eccentricities, perihelia near 35 AU, and semimajor axes greater than 50 AU. Using a maximum likelihood model, we estimate the total number of SKBOs larger than 100 km in diameter to be $N = (3.1^{+1.9}_{-1.3}) \times 10^4$ (1 σ errors) and the total mass of SKBOs to be $M \sim 0.05\ M_\oplus$, demonstrating that the SKBOs are similar in number and mass to the Kuiper Belt inside 50 AU.

Subject headings: comets: general — Kuiper Belt, Oort Cloud — solar system: formation

1. INTRODUCTION

The outer solar system is richly populated by small bodies in a thick trans-Neptunian ring known as the Kuiper Belt (Jewitt, Luu, & Chen 1996). It is widely believed that the Kuiper Belt objects (KBOs) are remnant planetesimals from the formation era of the solar system and are composed of the oldest, least modified materials in our solar system (Jewitt 1999). KBOs may also supply the short-period comets (Fernández & Ip 1983; Duncan, Quinn, & Tremaine 1988). The orbits of KBOs are not randomly distributed within the Belt but can be grouped into three classes. The classical KBOs constitute about two-thirds of the known objects and display modest eccentricities ($e \sim 0.1$) and semimajor axes (41 AU $< a <$ 46 AU) that guarantee a large separation from Neptune at all times. The resonant KBOs, which comprise most of the remaining known objects, are trapped in mean-motion resonances with Neptune, principally the 3 : 2 resonance at 39.4 AU. In 1996, we discovered the first example of a third dynamical class, the scattered KBOs (SKBOs): 1996TL$_{66}$ occupies a large ($a \sim 85$ AU), highly eccentric ($e \sim 0.6$), and inclined ($i \sim 25°$) orbit (Luu et al. 1997). It is the defining member of the SKBOs, characterized by large eccentricities and perihelia near 35 AU (Duncan & Levison 1997). The SKBOs are thought to originate from Neptune scattering, as evidenced by the fact that all SKBOs found to date have perihelia in a small range near Neptune (34 AU $< q <$ 36 AU).

In this Letter, we report preliminary results from a new survey of the Kuiper Belt undertaken at the Canada-France-Hawaii Telescope (CFHT) using a large-format charge-coupled device (CCD). This survey has yielded three new SKBOs. Combined with published results from an earlier survey (Jewitt, Luu, & Trujillo 1998) and with dynamical models (Duncan & Levison 1997), we obtain new estimates of the population statistics of the SKBOs. The main classes of KBOs appear in Figure 1, a plan view of the outer solar system.

[1] Based on observations collected at Canada-France-Hawaii Telescope, which is operated by the National Research Council of Canada, the Centre National de la Recherche Scientifique de France, and the University of Hawaii.

2. SURVEY DATA

Observations were made with the 3.6 m CFHT and 12,288 × 8192 pixel mosaic CCD (J.-C. Cuillandre, B. Starr, S. Isani, G. A. Luppino, & J. Tonry 1999, in preparation). Ecliptic fields were imaged within 1.5 hr of opposition to enhance the apparent sky-plane speed difference between the distant KBOs (~3″ hr^{-1}) and foreground main-belt asteroids ($\gtrsim$25″ hr^{-1}). Parameters of the CFHT survey are summarized in Table 1, in which they are compared with parameters of the survey earlier used to identify 1996TL$_{66}$ (Luu et al. 1997; Jewitt et al. 1998). We include both surveys in our analysis of the SKBO population.

Artificial moving objects were added to the data to quantify the sensitivity of the moving object detection procedure (Trujillo & Jewitt 1998). The seeing in the survey varied from 0.″7 to 1.″1 (FWHM). Accordingly, we analyzed the data in three groups based on the seeing. Artificial moving objects were added to bias-subtracted twilight sky-flattened images, with profiles matched to the characteristic point-spread function for each image group. These images were then passed through the data analysis pipeline. The detection efficiency was found to be uniform with respect to sky-plane speed in the 1″–10″ hr^{-1} range, with efficiency variations due only to object brightness.

The seeing-corrected efficiency function was fitted with a hyperbolic tangent profile for use in the maximum likelihood SKBO orbital simulation described in § 3:

$$\epsilon = \frac{\epsilon_{\max}}{2}\left[\tanh\left(\frac{m_{R50} - m_R}{\sigma}\right) + 1\right], \quad (1)$$

where $0 < \epsilon < 1$ is the efficiency at detecting objects of red magnitude m_R, $\epsilon_{\max} = 0.83$ is the maximum efficiency, $m_{R50} = 23.6$ is the magnitude at which $\epsilon = \epsilon_{\max}/2$, and $\sigma = 0.4$ mag is the characteristic range over which the efficiency drops from $\epsilon_{\max}$ to zero.

The orbital parameters of the four established SKBOs are listed in Table 2. It should be noted that the three most recent SKBOs have been observed for a time base of about 3 months, so their fitted orbits are subject to revision. However, the 4 yr

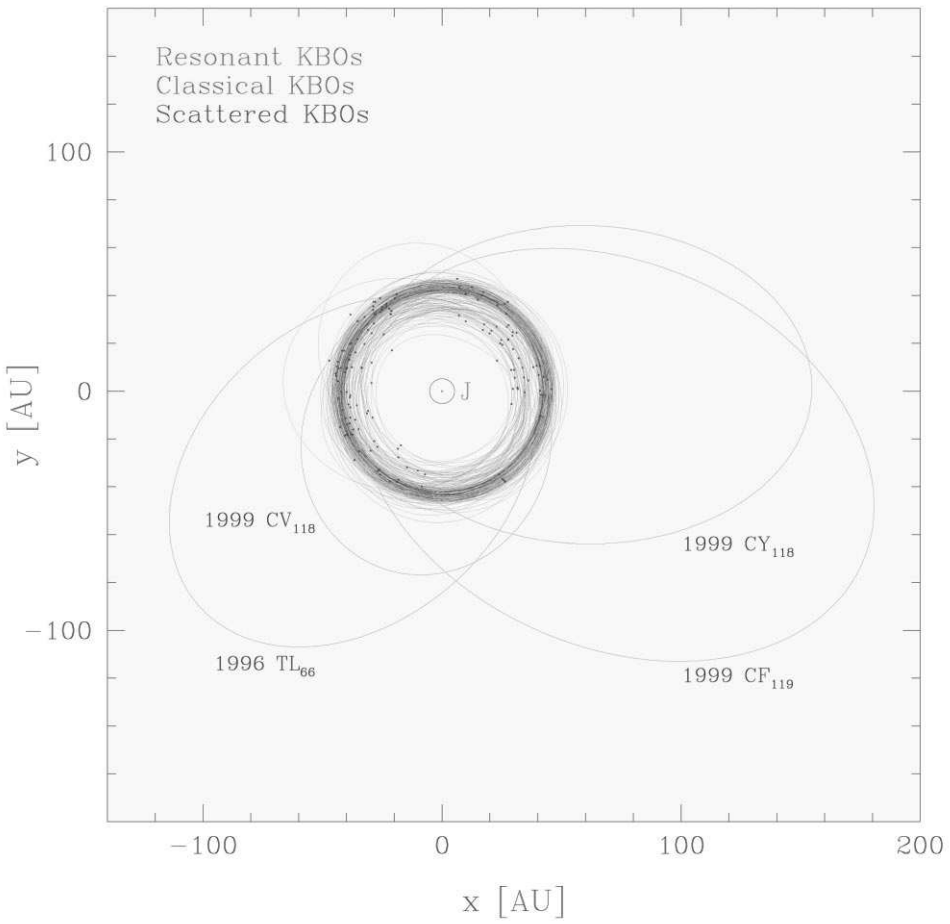

FIG. 1.—Plan view of the outer solar system; the green circle represents the orbit of Jupiter. Kuiper Belt objects have been color-coded based on their orbital classification. The four SKBO orbits are distinct.

orbit of 1996TL_{66} has changed very little since its initial announcement with a 3 month arc (a = 85.754, e = 0.594, i = 23.9, ω = 187.7, Ω = 217.8, M = 357.3, and epoch 1996 November 13; Minor Planet Electronic Circular 1997-B18). A plot of eccentricity versus semimajor axis appears in Figure 2, showing the dynamical distinction of SKBOs from the other KBOs. All SKBOs have perihelia 34 AU $< q <$ 36 AU. To avoid confusion with classical and resonant KBOs also having perihelia in this range, we concentrate on the SKBOs with semimajor axes $a > 50$ AU. In so doing, we guarantee that our estimates provide a solid lower bound to the true population of SKBOs.

TABLE 1
SURVEY PARAMETERS

QUANTITY	TELESCOPE	
	UH 2.2 m	CFHT 3.6 m
Focal ratio	f/10	f/4
Instrument	8k mosaic	12k × 8k mosaic
Plate scale (arcsec pixel^{-1})	0.135	0.206
Field area (deg^2)	0.09	0.33
Total area (deg^2)	51.5	20.2
m_{R50}[a]	22.5	23.6
θ[b] (arcsec)	0.8–1.0	0.7–1.1
Filter	*VR*[c]	*R*
Quantum efficiency	0.33	0.75
N_{SKBOs}[d]	1	3

[a] The red magnitude at which detection efficiency reaches half of the maximum efficiency.
[b] The typical FWHM of stellar sources for the surveys.
[c] The *VR* filter has a high transmission in the 5000–7000 Å range (Fig. 1 of Jewitt et al. 1996).
[d] The number of SKBOs detected.

3. POPULATION ESTIMATES

The number of SKBOs can be crudely estimated by simple extrapolation from the discovered objects. The faintest SKBO in our sample, 1999CY_{118}, was bright enough for detection only during the 0.24% of its ~1000 yr orbit spent near perihelion. Our 20.2 deg^2 of ecliptic observations represent ~1/500th of the total $\pm 15°$ thick ecliptic, roughly the thickness of the Kuiper Belt (Jewitt et al. 1996). Thus, we crudely infer the population of SKBOs to be of order $500/2.4 \times 10^{-3} \sim 2 \times 10^5$. To more accurately quantify the population, we use a maximum likelihood method to simulate the observational biases of our survey.

Our discovery of four SKBOs with the CFHT and University of Hawaii (UH) telescopes provides the data for the maximum likelihood simulation. We assess the intrinsic population of SKBOs by the following procedure (Trujillo 1999): (1) create a large number (~10^8) of artificial SKBO orbits drawn from an assumed distribution; (2) determine the ecliptic latitude,

TABLE 2
THE SKBOs[a]

Variable	$1996TL_{66}$	$1999CV_{118}$	$1999CY_{118}$	$1999CF_{119}$
Orbital Properties				
a (AU)	85.369	56.532	95.282	115
e	0.590	0.387	0.642	0.687
i (deg)	23.9	5.5	25.6	19.7
ω (deg)	184.5	126.6	21.4	218.1
Ω (deg)	217.8	305.6	163.1	303.4
M (deg)	359.2	22.5	356.4	354.3
Epoch (1999)	Aug 10	Mar 23	Mar 23	Mar 23
Discovery Conditions				
Date	1996 Oct 9	1999 Feb 10	1999 Feb 10	1999 Feb 11
R (AU)	35.2	39.7	38.6	42.2
m_R	20.9	23.0	23.7	23.0
$m_R(1, 1, 0)$	5.3	7.0	7.8	6.7
Diameter (km)	520	240	170	270

NOTE.—a, e, i, ω, Ω, and M represent the Keplerian orbital elements semimajor axis, eccentricity, inclination, argument of perihelion, longitude of the ascending node, and mean anomaly at the given epoch. R is the heliocentric distance; m_R is the red magnitude at discovery, and $m_R(1, 1, 0)$ is red magnitude at zero phase angle, geocentric distance = R = 1 AU, assuming a phase-darkening law for dark objects (Bowell et al. 1989). The diameter is derived assuming a geometric albedo of 4%.

[a] Orbital elements from B. Marsden 1999, private communication.

longitude, and sky-plane velocity of each artificial object using the equations of Sykes & Moynihan (1996; a sign error was found in eq. [2] of their text and corrected before use) and compute the object's brightness using the H, G formalism of Bowell et al. (1989), assuming an albedo of 0.04; (3) determine the detectability of each artificial object based on the detection efficiency and sky-area imaged in the two surveys; (4) create a histogram of "detected" artificial objects in a-e-i–radius space, with a bin size sufficiently small such that binning effects are negligible; (5) based on this histogram, compute the probability of finding the true, binned, observed distribution of the four SKBOs, assuming Poisson detection statistics; and (6) repeat the preceding steps, varying the total number of objects in the distribution (N) and the slope ($q' = 3, 4$) of the differential size distribution to find the model most likely to produce the observations. A full description of the model parameters is found in Table 3.

This model was designed to match the SKBO population inclination distribution, eccentricity distribution, and ecliptic plane surface density as a function of heliocentric distance, as found in the only published SKBO dynamical simulation to date, that of Duncan & Levison (1997). It should be noted that the results of the 4 billion yr simulations of Duncan & Levison (1997) were based on only 20 surviving particles, averaged over the last 1 billion yr of their simulation for improved statistical accuracy. The total number of objects and the size distribution of objects remained free parameters in our model.

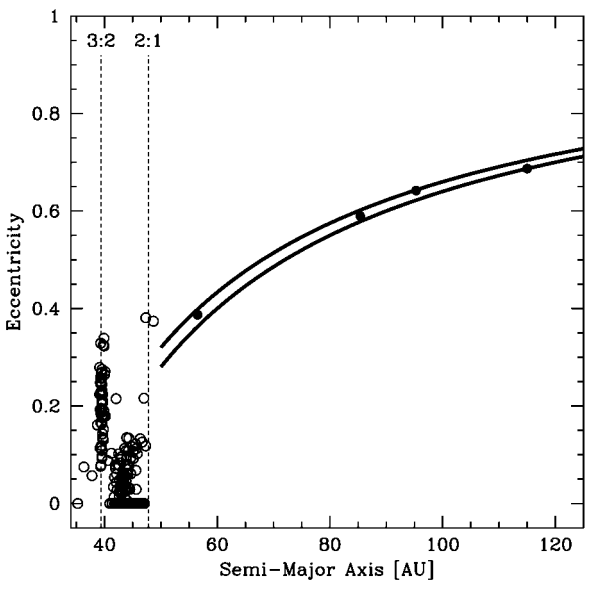

FIG. 2.—KBOs (*open circles*) and the four SKBOs (*filled circles*). The 3 : 2 and 2 : 1 resonances are shown as dashed lines. The solid lines represent perihelia of q = 34 and 36.

4. RESULTS

The results of the maximum likelihood simulation appear in Figure 3. Confidence levels were placed by finding the interval over which the integrated probability distribution corresponded to 68.27% and 99.73% of the total, hereafter referred to as 1 σ and 3 σ limits, respectively. The total number of SKBOs

TABLE 3
MODEL PARAMETERS

Variable	Value	Distribution	Description
a	50–200 AU	…[a]	Semimajor axis
e	0–1	Uniform	Eccentricity
i	0°–35°	Uniform	Inclination
ω	0°–360°	Uniform	Argument of perihelion
Ω	0°–360°	Uniform	Longitude of the ascending node
M	0°–360°	Uniform	Mean anomaly
r	50–1000 km	$n(r)dr \sim r^{-q'}dr$	Radius
q'	3, 4	…	Slope parameter
p_R	0.04	…	Red albedo
N	Free	…	Total number of objects
q	34–36 AU	…[b]	Perihelion distance

[a] Semimajor axis was chosen such that the surface density of objects vs. heliocentric distance follows $n(R) \sim R^{-p}\,dR$, where p = 2.5 (Duncan & Levison 1997).

[b] Perihelion distance was selected by first choosing a and then limiting e such that objects were in the 34–36 AU range.

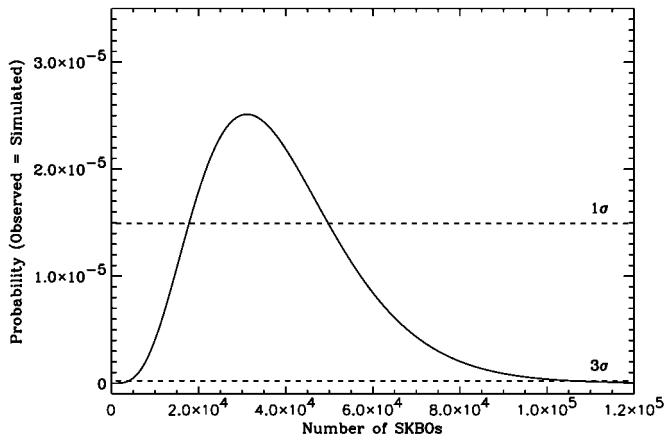

FIG. 3.—Probability that the model matches the observed distribution of SKBOs vs. the total number of objects in the model for the $q' = 4$ size distribution. The maximum likelihood is given by $N = (3.1^{+1.9}_{-1.3}) \times 10^4$ (1 σ). The dashed lines represent the 1 σ and 3 σ limits.

with radii between 50 and 1000 km is $N = (3.1^{+1.9}_{-1.3}) \times 10^4$ (1 σ) in the $q' = 4$ case, with $4.0 \times 10^3 < N < 1.1 \times 10^5$ 3 σ limits. The $q' = 3$ case is similar with $N = (1.4^{+1.1}_{-0.5}) \times 10^4$ (1 σ), with $2.0 \times 10^3 < N < 5.3 \times 10^4$ 3 σ limits. The $q' = 4$ and $q' = 3$ best fits are equally probable at the less than 1 σ level; however, we prefer the $q' = 4$ case because recent measurements of the Kuiper Belt support this value (Jewitt et al. 1998; Gladman et al. 1998; Chiang & Brown 1999). This population is similar in number to the Kuiper Belt interior to 50 AU, which contains about $\sim 10^5$ objects (Jewitt et al. 1998). The observation that only a few percent of KBOs are SKBOs is due to the fact that the SKBOs are only visible in magnitude-limited surveys during the small fraction of their orbits when near perihelion. In addition, the high perihelion velocities v of eccentric SKBOs may have implications for erosion in the Kuiper Belt since ejecta mass m_e scales with impact energy E as $m_e \sim E^2 \sim v^4$ (Fujiwara, Kamimoto, & Tsukamoto 1977).

Extrapolating the $q' = 4$ distribution to the size range 1 km $< r <$ 10 km yields $N \sim 4 \times 10^9$ SKBOs in the same size range as the observed cometary nuclei. This is comparable to the 10^9 needed for the SKBOs to act as the sole source of the short-period comets (Duncan & Levison 1997).

The total mass M of objects assuming $q' = 4$ is

$$M = 2.3 \times 10^{-3} p_R^{3/2} \frac{\rho}{(\text{kg m}^{-3})} \log\left(\frac{r_{\max}}{r_{\min}}\right) M_\oplus, \qquad (2)$$

where red geometric albedo $p_R = 0.04$, density $\rho = 2000$ kg m^{-3}, the largest object $r_{\max} = 1000$ km (Pluto-sized), and smallest object $r_{\min} = 50$ km yields $M \sim 0.05\ M_\oplus$, where $M_\oplus = 6 \times 10^{24}$ kg is the mass of the Earth. This is comparable to the total mass of the classical and resonant KBOs (0.2 $M_\oplus$; Jewitt et al. 1998). If only 1% of SKBOs have survived for the age of the solar system (Duncan & Levison 1997), then an initial population of 10^7 SKBOs (50 km $< r <$ 1000 km) and a SKBO primordial mass $\gtrsim 5\ M_\oplus$ are inferred.

Since our observations are concentrated near the ecliptic, we expected most of the discovered objects to have low inclinations. However, of the four established SKBOs, three have high inclinations ($i \gtrsim 20°$). The possibility of a Gaussian distribution of inclinations centered at $i \sim 20°$ was tested; however, the fit was not better than the uniform i case at the ≥ 3 σ level. If the SKBO inclinations were drawn from the Gaussian distribution, the total numbers of SKBOs reported here would be enhanced by a factor ~ 2. Combining this model-dependent uncertainty, the orbital uncertainties of the four SKBOs, and the computed Poisson noise, we estimate that our predictions provide an order-of-magnitude constraint on the population of the SKBOs. As additional SKBOs become evident in our continuing survey and as recovery observations of the SKBOs are secured, we will refine this estimate.

5. SUMMARY

We have constrained the SKBO population using surveys undertaken on Mauna Kea with two CCD mosaic cameras on two telescopes. The surveys cover 20.2 deg^2 to limiting red magnitude 23.6 and 51.5 deg^2 to limiting red magnitude 22.5. We find the following:

1. The SKBOs exist in numbers comparable to the KBOs. The observations are consistent with a population of $N = (3.1^{+1.9}_{-1.3}) \times 10^4$ (1 σ) SKBOs in the radius range 50 km $< r <$ 1000 km with a differential power-law size distribution exponent of $q' = 4$.
2. The SKBO population in the size range of cometary nuclei is large enough to be the source of the short-period comets.
3. The present mass of the SKBOs is approximately 0.05 $M_\oplus$. When corrected for depletion inferred from dynamical models (Duncan & Levison 1997), the initial mass of SKBOs in the early solar system approached 5 $M_\oplus$.

We are continuing our searches for these unusual objects because it is clear that they play an important role in outer solar system dynamics.

We thank Ken Barton for help at the Canada-France-Hawaii Telescope. This work was supported by a grant to D. C. J. from NASA.

REFERENCES

Bowell, E., Hapke, B., Domingue, D., Lumme, K., Peltoniemi, J., & Harris, A. 1989, in Asteroids II, ed. R. Binzel, T. Gehrels, & M. Matthews (Tucson: Univ. Arizona Press), 524
Chiang, E. I., & Brown, M. E. 1999, AJ, 118, 1411
Duncan, M. J., & Levison, H. F. 1997, Science, 276, 1670
Duncan, M., Quinn, T., & Tremaine, S. 1988, ApJ, 328, L69
Fernández, J. A., & Ip, W.-H. 1983, Icarus, 54, 377
Fujiwara, A., Kamimoto, G., & Tsukamoto, A. 1977, Icarus, 31, 277
Gladman, B., Kavelaars, J. J., Nicholson, P. D., Loredo, T. J., & Burns, J. A. 1998, AJ, 116, 2042
Jewitt, D. 1999, Ann. Rev. Earth Planet. Sci., 27, 287
Jewitt, D., Luu, J., & Chen, J. 1996, AJ, 112, 1225
Jewitt, D., Luu, J., & Trujillo, C. 1998, AJ, 115, 2125
Luu, J., Marsden, B. G., Jewitt, D., Trujillo, C. A., Hergenrother, C. W., Chen, J., & Offutt, W. B. 1997, Nature, 387, 573
Sykes, M. V., & Moynihan, P. D. 1996, Icarus, 124, 399
Trujillo, C. 1999, in Minor Bodies in the Outer Solar System ed. A. Fitzsimmons, R. West, & D. Jewitt (Heidelberg: Springer), in press
Trujillo, C., & Jewitt, D. 1998, AJ, 115, 1680